Journal of Microscopy, Vol. 214, Pt 1 April 2004, pp. 36–42
Received 2 September 2003; accepted 24 November 2003

Low-cost, frequency-domain, fluorescence lifetime confocal microscopy

M. J. BOOTH & T. WILSON
Department of Engineering Science, University of Oxford, Parks Road, Oxford OX1 3PJ, U.K.

Key words. Confocal microscopy, fluorescence lifetime, laser diode, quadrative demodulation.

Summary

We describe the theory and implementation of a frequency-domain fluorescence lifetime confocal microscope using switched diode laser illumination. Standard, communications-type, radio-frequency electronics are used to provide inexpensive modulation references and to perform phase-sensitive detection. This allows the rapid acquisition of fluorescence intensity and lifetime images and their display in real time. We show fluorescence lifetime images of bead objects and fluorescence lifetime images of biological specimens from a single confocal scan.

1. Introduction

Three-dimensionally resolved fluorescence microscopy is an invaluable tool in the biological sciences permitting the high-resolution imaging of cellular structures and processes. Combination of such techniques with the measurement of fluorescence dynamics provides further capabilities, for example the ability to distinguish fluorophores differing in fluorescence lifetime but showing similar spectral properties (Lakowicz, 1999). Such three-dimensional (3D) fluorescence lifetime microscopy (FLIM) has further applications. The Ångström-scale proximity of fluorescently labelled bodies can be probed by measuring the effect of Förster resonance energy transfer (FRET) on the fluorescence lifetime. Furthermore, the fluorescence dynamics are influenced by ion concentrations, pH, viscosity and refractive index, all of which can provide extra imaging information (Lakowicz, 1999).

After a fluorophore absorbs a photon of appropriate wavelength, it enters an excited state from which it can emit a longer wavelength fluorescence photon. The time delay between excitation and emission follows a statistical distribution. If one considers a large number of excitation events, whether through the simultaneous excitation of a large number of fluorophores or through appropriate time-averaging of the emission from a small number, the fluorescence dynamics behave as a linear system that can be fully described by an impulse response or a frequency transfer function. Fluorescence lifetime measurements can generally be classified as time domain or frequency domain and the approaches are analogous to measuring this impulse response and frequency transfer function. In the time-domain approach, the fluorophore is excited by a short pulse of light (the impulse) and one observes the form of the statistical decay curve (the impulse response) at a sequence of time steps. In the frequency-domain approach, the excitation light is modulated at an appropriate frequency and the effects of the fluorescence dynamics manifest themselves in the phase shift and change in modulation depth between the excitation and emission light. A sequence of measurements at different frequencies provides the full transfer function. For mono-exponential fluorescence decays, however, the decay time constant (often referred to simply as the fluorescence lifetime) is readily obtained from a measurement at a single frequency. Indeed, this quantity alone is often used to characterize the fluorescent species. More complex decay characteristics can be represented by two or more exponential decays and their corresponding lifetime components.

Three-dimensional resolution in microscopy can be implemented in point-scanning or wide-field systems. The confocal microscope is a point-scanning microscope that provides 3D resolution by using a pinhole to prevent out-of-focus emission from reaching the detector (Wilson, 1990). The volume image is then compiled by scanning along three axes. Two-photon excitation fluorescence microscopy is a point-scanning method that also demonstrates 3D resolution, albeit not requiring the use of a pinhole because the fluorescence emission is confined to the focal spot (Denk *et al.*, 1990). Both of these methods have been used in 3D-FLIM applications (Carlsson & Liljeborg, 1997; Schönle *et al.*, 2000). Wide-field optical sectioning techniques can provide 3D resolution comparable with that of the confocal microscope in a wide-field microscope system (Juskaitis *et al.*, 1996; Neil *et al.*, 1998). One such method, using structured illumination, has been combined with both frequency-domain (unpublished results) and time-domain FLIM (Cole *et al.*, 2000).

Time-domain methods typically require a short pulsed illumination source, such as titanium sapphire lasers or laser

Correspondence to: Martin Booth. Fax: +44 (0)1865 273905; e-mail: martin.booth@eng.ox.ac.uk

diodes. In wide-field imaging this has been used with time-gated detection using a gated intensifier with a CCD camera. For point-scanning systems time-correlated single photon counting (TCSPC) has been used (Becker *et al.*, 1999). TCSPC has also been demonstrated in wide-field imaging (Emiliani *et al.*, 2003). Frequency-domain methods require the modulation of the illumination source either directly, as with a modulated diode laser, or using an electro- or acousto-optic modulator. Detection in frequency-domain point scanning systems can be implemented through phase-sensitive lock-in detection. In wide-field imaging systems, both gated intensifiers/CCD cameras (Schneider & Clegg, 1997; Cole *et al.*, 2000) and modulated CCD cameras (Mitchell *et al.*, 2002) have been demonstrated.

Many of the previously reported methods have operated at a limited speed. For example, this could be a consequence of dead time in the detection electronics, such as in TCSPC. After a photon is detected, there is a period of time (the dead time) during which another photon cannot be registered. In order not to lose photons in this manner, the general approach is to reduce the intensity of the illumination, thus increasing the mean arrival time between photons and consequently increasing the total time required to acquire an image. As another example, the time-gated detection methods are relatively inefficient in the use of available photons because only those photons arriving during the gate period can contribute to the image. Moreover, the intensification process introduces noise, which necessitates longer averaging. For FLIM to function reliably it is essential that the specimen remain stationary over time scales similar to that over which the acquisition takes place. Unwanted movement of the specimen can lead to artefacts and misleading lifetime measurements. This effect was clearly illustrated by Hanley *et al.* (2001). For FLIM of dynamic processes, it is therefore desirable to have a system that can make measurements of fluorescence lifetimes on time scales similar to the normal acquisition time of each image component, whether a frame in wide-field methods or a pixel in point-scanning methods (Schneider & Clegg, 1997).

It is interesting to note that relatively little attention has been given to the frequency-domain approach in point-scanning systems. This is possibly due to the perceived expense of laboratory-grade lock-in amplifier/detectors operating in the radio frequency (RF) range usually required for the measurement of nanosecond and subnanosecond fluorescence lifetimes (Harms *et al.*, 1999). However, the ubiquity of modern mobile communications has led to the development of highly optimized and inexpensive RF electronic components that are ideally suited to the phase-sensitive detection of these RF signals. We present in this paper a fluorescence lifetime confocal microscope with violet diode laser illumination incorporating such detector electronics. The system was optimized to give rapid pixel by pixel measurement of the phase lifetime at an appropriate modulation frequency making efficient use of the available fluorescence photons.

2. Frequency-domain fluorescence lifetime measurement with switched illumination

The microscope we describe in this paper uses switched laser diode illumination and performs frequency-domain fluorescence lifetime measurements at the fundamental frequency of the switched waveform. The lifetime information is extracted from the fundamental modulated component of the fluorescence emission using an RF receiver comprising a superheterodyne mixer and quadrature demodulator. In this section we describe the theory of operation of this system.

In its most straighforward implementation, frequency-domain FLIM involves illumination of the specimen with light sinusoidally modulated at an appropriate angular frequency, given by $\omega = 2\pi/T$ where T is the period. As a function of time, t, the illumination intensity at the specimen is thus

$$I_{ill} = K\left[\frac{1}{2} + \frac{1}{2}\cos(\omega t)\right]. \quad (1)$$

This is illustrated in Fig. 1(a). K is maximum illumination intensity and the modulation depth has been chosen so that the full range of intensity is used. If we instead consider an illumination source that, rather than being modulated sinusoidally, is switched on and off according to the scheme in Fig. 1(b), the illumination intensity at the specimen can be expressed as a Fourier series:

$$I_{ill} = K\left[\frac{\alpha}{\pi} + \frac{2}{\pi}\sum_{n=1}^{\infty}\frac{1}{n}\sin(n\alpha)\cos(n\omega t)\right]. \quad (2)$$

It can be seen that the illumination contains an infinite number of harmonics of the fundamental frequency, ω. Any of these harmonics could be independently used for fluorescent lifetime measurements. By choosing the value of α, i.e. the

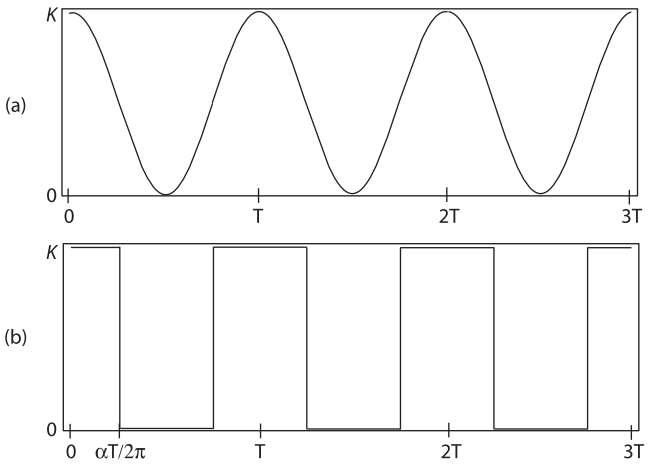

Fig. 1. (a) Illumination intensity as a function of time for sinusoidal modulation. (b) Illumination intensity as a function of time for switched illumination.

proportion of the period that the illumination is on, we can control the amplitudes of the harmonics present in the waveform. For example, when $\alpha = \pi/2$ the amplitude of the fundamental has the maximum value of $2K/\pi$. It is interesting to note that this amplitude is greater than the equivalent term in Eq. (1) by a factor of $4/\pi \approx 1.27$. In effect, by switching the illumination in this manner, rather than modulating it sinusoidally over the same intensity range, we can increase the energy in the fundamental frequency component.

From now on, we consider only the fundamental component. We can therefore write Eq. (2) as

$$I_{ill} = \frac{K}{\pi}[\alpha + 2 \sin \alpha \cos(\omega t)] + O(2\omega), \tag{3}$$

where the final term represents the higher harmonics. The emitted fluorescence can then be represented by

$$I_{em} = \frac{K}{\pi}[\alpha A + 2B \sin \alpha \cos(\omega t - \phi)] + O(2\omega), \tag{4}$$

where ϕ is the phase shift and the values A and B represent the change in magnitude of the constant and modulated components, respectively. We now assume this is measured by a photodetector that emits a voltage signal proportional to the fluorescence emission. The signal is filtered to extract the low-frequency and fundamental components, which are processed separately. The low-frequency signal, corresponding the standard fluorescence intensity image, is amplified by a gain G_0 to give the signal

$$V_0 = G_0 \alpha A K/\pi. \tag{5}$$

The gain also incorporates any losses introduced by the filters. The fundamental signal is amplified by a gain G_1 to give the signal

$$V_1 = \frac{2G_1BK}{\pi} \sin \alpha \cos(\omega t - \phi - \delta), \tag{6}$$

where δ is the total phase delay introduced by the optical and electronic system. This phase delay was measured with the calibration step described below. The phase lifetime, τ_ϕ, is conventionally calculated from the phase shift ϕ as (Lakowicz, 1999)

$$\tau_\phi = \frac{1}{\omega} \tan \phi. \tag{7}$$

The present system uses the standard RF electronics technique of coherent superheterodyne demodulation in order to find the phase ϕ. Modern components have been highly optimized to perform such demodulation and their internal processes can be complex. However, the overall operation is such that the demodulator generates two low-frequency baseband signals known as the 'in-phase' (I) and 'quadrature' (Q) signals. In communications systems, different signals can be independently encoded on to the I and Q channels. In the fluorescence lifetime microscope, these channels are intrinsically linked to the phase shift ϕ because they represent the proportion of the modulated fluorescence signal in phase and out of phase with the laser modulation reference. In effect, the demodulator multiplies the input signal of Eq. (6) by $\cos(\omega t)$ giving

$$\frac{G_1BK}{\pi} \sin \alpha [\cos(\phi + \delta) + \cos(2\omega t - \phi - \delta)]. \tag{8}$$

The high frequency 2ω is then removed using a low-pass filter to give the output signal for the I channel as

$$V_I = \frac{G_1BK}{\pi} \sin \alpha \cos(\phi + \delta) + V_{I0}, \tag{9}$$

where V_{I0} is a constant offset voltage. The output for the Q channel is effectively produced through multiplying the input signal by $\sin(\omega t)$ to give

$$\frac{G_1BK}{\pi} \sin \alpha [\sin(\phi + \delta) + \sin(2\omega t - \phi - \delta)], \tag{10}$$

which, when filtered in a similar manner, gives the output signal

$$V_Q = \frac{G_1BK}{\pi} \sin \alpha \sin(\phi + \delta) + V_{Q0}, \tag{11}$$

where V_{Q0} is a constant offset voltage. The phase lifetime could therefore be extracted from these signals using the relationship

$$\tau_\phi = \frac{1}{\omega} \tan\left[\tan^{-1}\left(\frac{\hat{V}_Q}{\hat{V}_I}\right) - \delta\right], \tag{12}$$

where we define $\hat{V}_I = V_I - V_{I0}$ and $\hat{V}_Q = V_Q - V_{Q0}$. However, we employed the following equivalent formulation because it is more robust for numerical calculation:

$$\tau_\phi = \frac{1}{\omega} \cdot \frac{\hat{V}_Q \cos\delta - \hat{V}_I \sin\delta}{\hat{V}_I \cos\delta - \hat{V}_Q \sin\delta}. \tag{13}$$

The modulation lifetime is conventionally defined as (Lakowicz, 1999)

$$\tau_m = \frac{1}{\omega}\sqrt{\frac{1}{m^2} - 1}, \tag{14}$$

where m is the relative modulation depth between the excitation and emission. Again, the modulation depth can be calculated using the I and Q outputs. In the present system we can derive this as

$$m = C\frac{\sqrt{\hat{V}_I^2 + \hat{V}_a^2}}{V_0}, \tag{15}$$

where the constant C is given by

$$C = \frac{G_0\alpha}{G_1 \sin\alpha}. \tag{16}$$

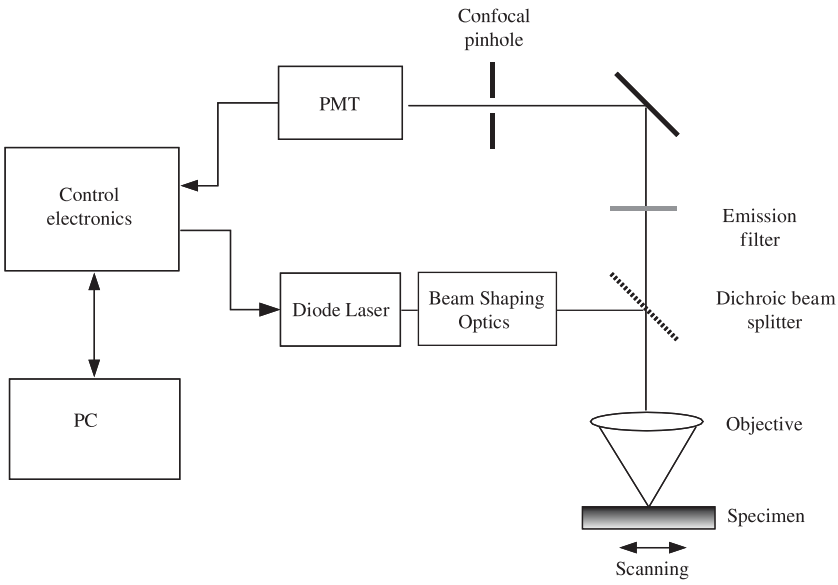

Fig. 2. Schematic diagram of the fluorescence lifetime confocal microscope.

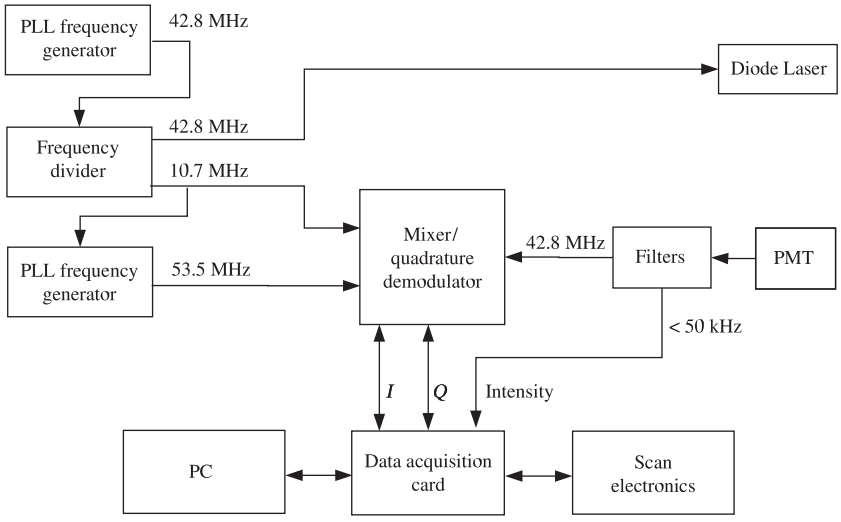

Fig. 3. Schematic of the fluorescence lifetime confocal microscope control and detection electronics.

Calculation of τ_m therefore requires explicit knowledge of C. This was found through the calibration step described below. For mono-exponential decays $\tau_\phi = \tau_m$ and in general $\tau_\phi < \tau_m$ (Lakowicz, 1999).

3. Experimental details

The incorporation of our fluorescence lifetime measurement system required minimal modification of an existing confocal microscope. A schematic diagram of the optical set-up is shown in Fig. 2. Illumination was provided by a 415 nm wavelength violet laser diode (Picoquant LDH C-400) driven by a fast switched diode laser driver (Picoquant FSL 500) synchronized to an external reference such that the illumination was on for 8.2 ns of the 23.4 ns period, equivalent to $\alpha = 0.37\pi$. The beam was passed through beam conditioning optics, comprising an anamorphic prism pair and an astigmatic correction lens, before being focused through a pinhole to obtain a clean mode shape. The objective lens (Olympus U-Apo 340, 40×, 1.35 NA oil-immersion, UV corrected) focused the illumination into the specimen, which was mounted on a stage scanner. The fluorescence was collected by the same lens and passed through a dichroic filter and emission filter that blocked wavelengths shorter than 435 nm. The fluorescence light was focused by a tube lens (focal length 180 mm) on to a confocal pinhole, with a diameter of 20 μm, which was placed in front of a photomultiplier tube (Hamamatsu, H6780-01).

A schematic of the detection electronics is shown in Fig. 3. The phase-sensitive detection was implemented using an RF quadrature demodulator receiver module (Analog Devices, AD607), which operates on the principle of superheterodyne coherent detection. This requires two phase-locked signals for demodulation, a local oscillator (LO) reference and an intermediate frequency (IF) reference. The IF is the fixed frequency

for which a demodulator stage is optimized, which in this case was 10.7 MHz. The modulation frequency can, in theory, be set to any value as long as the difference between it and the LO frequency is equal to the IF. We chose a modulation frequency of 42.8 MHz and, hence, an LO frequency of 53.5 MHz. This was convenient because the IF could be simply derived from the modulation frequency using a divide-by-four frequency divider. A reference signal at 42.8 MHz was provided by a phase-locked loop (PLL) frequency generator (Analog Devices, AD4116). This signal was input into a programmable frequency divider (Dallas Semiconductor, DS1075) configured to generate phase-locked square wave outputs. The first output was at the input frequency, 42.8 MHz, and was used as the modulation signal for the laser. The second output was at one-quarter of the input frequency, 10.7 MHz, and provided the IF reference for the receiver. The 10.7 MHz output was also used as the reference for a second PLL frequency generator that produced a 53.5 MHz LO signal.

The photomultiplier output signal was preamplified using a high-speed operational amplifier (Analog Devices, AD8001), configured as a ×10 non-inverting amplifier, then split into low-frequency (< 10 MHz) and high-frequency (> 10 MHz) components using passive, matched LC filters. The low-frequency signal was further amplified and filtered to a bandwidth of 50 kHz, corresponding to the maximum pixel sampling rate. This signal corresponded to the standard fluorescence intensity. The high-frequency signal, containing the fundamental at 42.8 MHz and higher harmonics, was used as the input to the RF receiver. Although present at the input to the receiver, the higher harmonics were efficiently removed because of the 2 MHz bandwidth of the IF amplification stage in the quadrature demodulator and therefore they had no effect on the output. Like the fluorescence intensity signal, the I and Q outputs of the quadrature demodulator stage were filtered to the bandwidth of 50 kHz. The three filtered signals (I, Q and intensity) were sampled with 12-bit resolution by the data acquisition card (Adlink, PCI9118DG) in the PC. The data acquisition was synchronized with a pixel clock generated by the stage-scanning electronics. The three signals were readily processed using custom software to calculate the phase shift, modulation and the corresponding lifetime values. This allowed real-time simultaneous observation of both fluorescence intensity and lifetime. When required, averaging of frames was also implemented by the sequential averaging of the I, Q and intensity channels.

Calibration of the system required finding the values of the offset voltages on the I and Q channels, V_{I0} and V_{Q0}, the offset phase δ and the modulation constant C. This proceeded as follows. First, V_{I0} and V_{Q0} were measured by taking the average pixel values during a scanned frame when the laser was switched off. The offset phase δ was found by placing a plane mirror specimen in the object plane and removing the emission filter. Sufficient reflected light was transmitted by the dichroic filter to generate a signal from the photomultiplier. δ was taken as the mean phase of this signal. This configuration was also used to ascertain C as the ratio of the average of the intensity signal to the average of the modulation signal, as calculated from the I and Q channels. Because C was dependent upon the gains G_0 and G_1 and upon α, the calibration was repeated whenever any of these values were adjusted.

4. Experimental results

A specimen containing two different types of fluorescent beads was prepared by mixing a suspension of beads with a 1-μm nominal diameter (Molecular Probes Fluospheres, 430 nm/465 nm excitation/emission maxima) and beads with a 2-μm nominal diameter (Molecular Probes Fluospheres, 505 nm/515 nm excitation/emission maxima). The suspension was allowed to dry on a cover glass so that the beads adhered to the surface. The specimen was then mounted in immersion oil and fixed to a microscope slide. Example images are shown in Fig. 4. The fluorescence intensity image is shown in Fig. 4(a). Figure 4(b,c) show, respectively, the phase lifetime, τ_ϕ, and the modulation lifetime, τ_m. In these images, the hue represents the lifetime, according to the 0–6 ns scale shown, and the brightness represents the fluorescence intensity. Each image was derived from the average of four confocal scans as described above; this was a total scan time of approximately 15 s. The difference in fluorescence lifetime between the two types of beads can be clearly seen. The phase lifetime of each fluorophore was measured by taking the average over one bead of each type. The phase lifetime of the smaller beads was found to be 2.01 ns, whereas for the larger beads this was found to be 3.66 ns. The corresponding values of modulation lifetime were 2.44 ns and 3.18 ns. Normally, it would be expected that for simple exponential decays $\tau_\phi = \tau_m$. For multi-exponential decays, one should expect that $\tau_\phi > \tau_m$. We note that in this case the relationship was not satisfied for the larger beads. This can be explained by the fact that there was a small but noticeable dependence of the modulation lifetime on the intensity, as seen in Fig. 4(c). This was a consequence of the sensitivity of this particular measurement to the gain balance of the I, Q and intensity channels, and the offset calibration. The measurement of τ_m could, of course, be made more reliable through the careful design optimization of the intensity channel amplification. However, because the measurement of τ_ϕ depended only on the optimized and balanced I and Q signals from the RF demodulator, we chose to use this more robust measurement to demonstrate the operation of the system.

Figure 5 shows combined fluorescence intensity and phase lifetime images of *Nicotiana tabacum* specimens. These specimens were labelled with green fluorescent protein (GFP) and also showed significant autofluorescence. The specimens were immersed in water and secured with a cover glass and were imaged using an Olympus U-Apo 340, 1.15 NA water-immersion lens. The images shown were acquired in a single confocal scan of duration 4 s. Considerable variations in

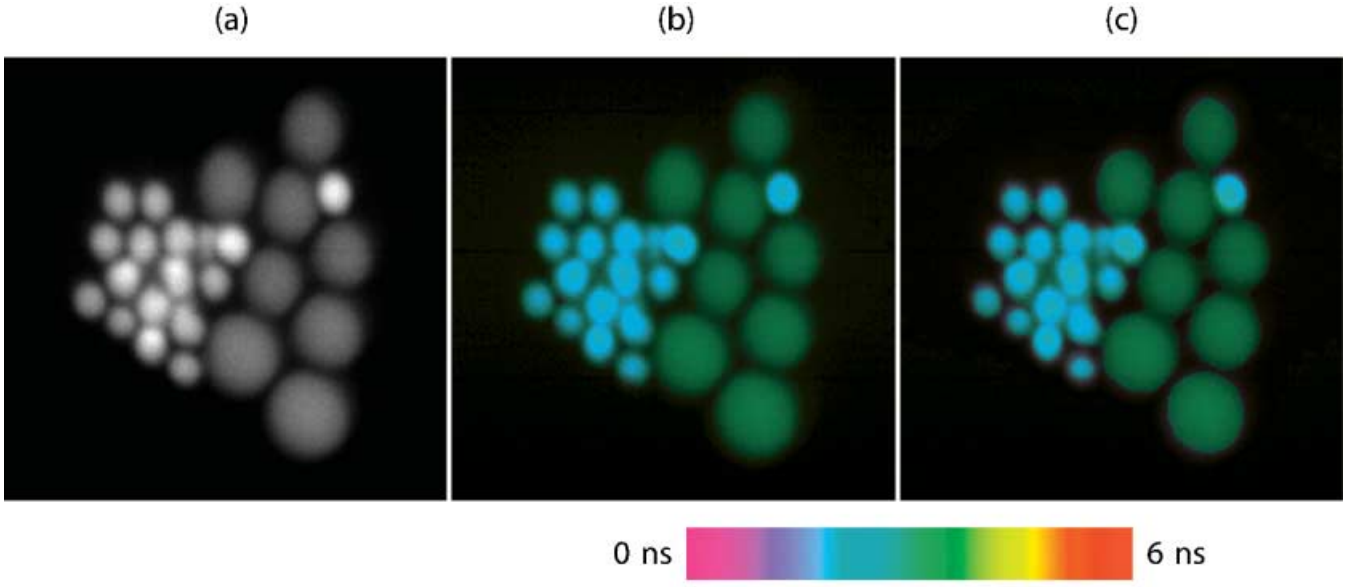

Fig. 4. Fluorescence intensity and lifetime images of a specimen containing 1 μm and 2 μm beads labelled with different fluorophores: (a) the fluorescence intensity, (b) the phase lifetime and (c) the modulation lifetime. The hue of images (b) and (c) represents the fluorescence lifetime corresponding to the scale shown from 0 to 6 ns. The image width is 15 μm.

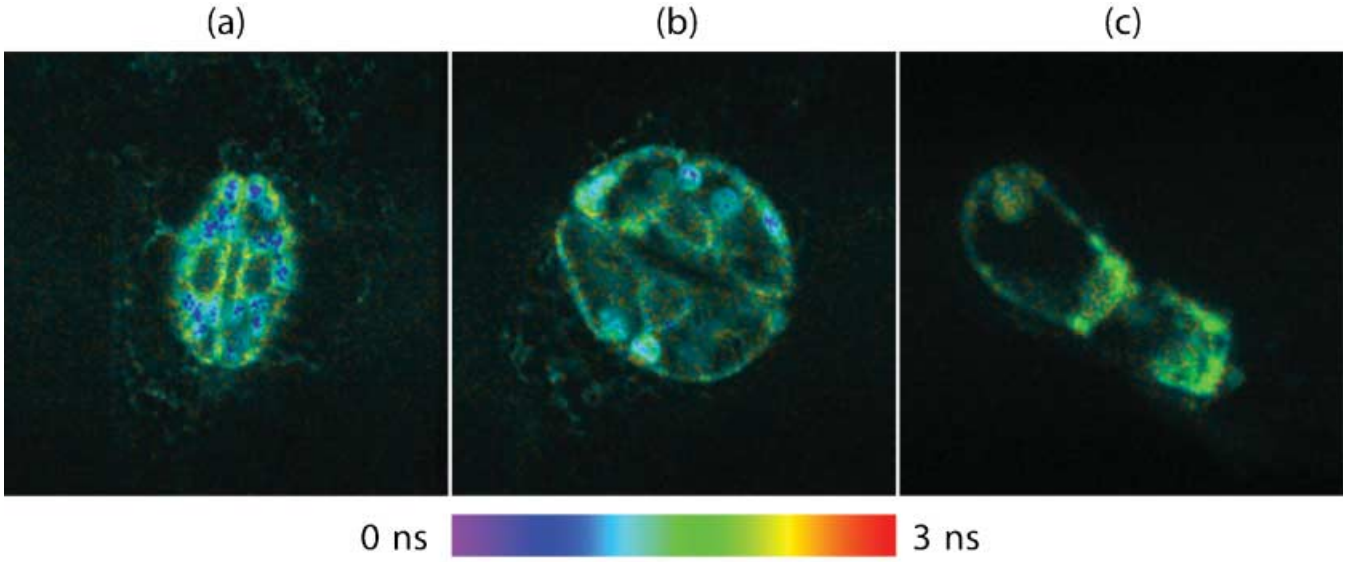

Fig. 5. Combined fluorescence intensity and phase lifetime images of *Nicotiana tabacum* specimens. The fluorescence is a combination of autofluorescence and GFP fluorescence. (a,b) Stomata of leaves in which the endoplasmic reticulum was labelled with GFP5. (c) A trichrome of a leaf with GFP5-labelled Golgi. The hue of the images represents the fluorescence lifetime corresponding to the scale shown from 0 to 3 ns. The image widths are: (a) 100 μm, (b) 70 μm, (c) 65 μm.

fluorescence lifetime are apparent in the images. The lifetimes of < 1 ns correspond to the chloroplasts, which are known to have short fluorescence lifetimes (Holub *et al.*, 2000). Other parts of the specimen, where autofluorescence from the cell walls and GFP is excited, show longer lifetimes in the range of approximately 2–3 ns. Reports have shown that the fluorescence lifetimes of GFP variants are typically around 3 ns depending upon exact conditions (Hanley *et al.*, 2001).

5. Discussion

We have demonstrated a method using modulated diode laser illumination and readily available communications-type RF electronics for obtaining fluorescence lifetime measurements concurrently with fluorescence intensity images in a confocal microscope. This method is complementary to the presently available methods and permits the rapid measurement of

single real or apparent lifetime components. Because the measurement accuracy depends ultimately on the number of detected photons, we made this possible by using switched illumination with a high duty cycle and phase-sensitive detection that used all photons detected by the photomulitplier tube. We have been able to measure fluorescence lifetimes during a single confocal scan lasting 4 s. This scan time was limited by the speed of the available scanning stage and could be reduced further. Such increases in speed are an important factor when imaging dynamic processes in specimens. The component cost of the demodulation electronics was considerably less than commercially available fluorescence lifetime measurement products. Adaptation of the demodulation system could allow simultaneous phase measurement at several frequencies corresponding to harmonics of the switching frequency. These harmonics could be controlled according to Eq. (2) by adjusting the duty cycle of the illumination. It could also be possible simultaneously to measure non-harmonic components by using more complex modulation schemes.

Acknowledgements

This work was supported by the Biotechnology and Biological Sciences Research Council (U.K.). We are grateful to Professor B. Vojnovic of the Gray Cancer Institute, Mount Vernon Hospital, for the loan of the photomultiplier. The *Nicotiana tabacum* specimens were kindly provided by Professor C. Hawes and Dr F. Brandizzi of the School of Biological and Molecular Sciences, Oxford Brookes University.

References

Becker, W., Hickl, H., Zander, C., Drexhage, K.H., Sailer, M., Sithert, S. & Wolfrum, J. (1999) Time-resolved detection and identification of single analyte molecules in microcapillaries by time-correlated single-photon counting (tcspc). *Rev. Sci. Instrum.* **70**, 1835–1841.

Carlsson, K. & Liljeborg, A. (1997) Confocal fluorescence microscopy using spectral and lifetime information to simultaneously record four fluorophores with high channel separation. *J. Microsc.* **185**, 37–46.

Cole, M.J., Siegel, J., Webb, S.E.D., Jones, R., Dowling, K., French, P.M.W., Lever, M.J., Sucharov, L.O.D., Neil, M.A.A., Juskaitis, R. & Wilson, T. (2000) Whole-field optically sectioned fluorescence lifetime imaging. *Opt. Lett.* **25**, 1361–1363.

Denk, W.-J., Strickler J.P. & Webb, W.W. (1990) Two-photon laser scanning fluorescence microscopy. *Science*, **248**, 73–76.

Emiliani, V., Sarivitto, D., Trannier, M., Piolot, T., Petrasek, Z., Kemnitz, K., Durieux, C. & Coppey-Moisan, M. (2003) Low-intensity two-dimensional imaging of fluorescence lifetimes in living cells. *Appl. Phys. Lett.* **83**, 2471–2473.

Hanley, Q.S., Subramaniam, V., Arndt-Jovin, D.J. & Jovin, T.M. (2001) Fluorescence lifetime imaging: multi-point calibration, minimum resolvable differences and artifact suppression. *Cytometry*, **43**, 248–260.

Harms, P., Sipior, J., Ram, N., Carter, G.M. & Rao, G. (1999) Low cost phase-modulation measurements of nanosecond fluorescence lifetimes using a lock-in amplifier. *Rev. Sci. Instrum.* **70**, 1535–1539.

Holub, O., Seufferheld, M.J., Gohlke, C., Govindjee, G. & Clegg, R.M. (2000) Fluorescence lifetime imaging (FLI) in real-time – a new technique in photosynthesis research. *Photosynthetica*, **38**, 581–599.

Juskaitis, R., Wilson, T., Neil, M.A.A. & Kozubek, M. (1996) Efficient real-time confocal microscopy with white light sources. *Nature*, **383**, 804–806.

Lakowicz, J.R. (1999) *Principles of Fluorescence Spectroscopy*, 2nd edn. Kluwer/Plenum, New York.

Mitchell, A.C., Wall, J.E., Murray, J.G. & Morgan, C.G. (2002) Direct modulation of the effective sensitivity of a CCD detector: a new approach to time-resolved fluorescence imaging. *J. Microsc.* **206**, 225–232.

Neil, M.A.A., Juskaitis, R. & Wilson, T. (1998) Real time 3d fluorescence microscopy by two beam interference illumination. *Opt. Commun.* **153**, 1–4.

Schneider, P.C. & Clegg, R.M. (1997) Rapid acquisition, analysis, and display of fluorescence lifetime-resolved images for real-time applications. *Rev. Sci. Instrum.* **68**, 4107–4118.

Schönle, A., Glatz, M. & Hell, S.W. (2000) Four-dimensional multiphoton microscopy with time-correlated single-photon counting. *Appl. Opt.* **39**, 6306–6311.

Wilson, T. (1990) *Confocal Microscopy*. Academic Press, London.